ELSEVIER

Journal of Chromatography A, 793 (1998) 77–90

JOURNAL OF CHROMATOGRAPHY A

Chiral separation of 3-phenyl-3-(2-pyridyl)propylamines, and analogous guanidines and guanidine-N-carboxylic acid esters with high-performance liquid chromatography and capillary zone electrophoresis[1]

Andreas Schuster[a], Günther Bernhardt[a], Ernst Eibler[b], Armin Buschauer[a,*], Willy Hesselink[c]

[a]*Institut für Pharmazie, Universität Regensburg, Universitätsstrasse 31, D-93040 Regensburg, Germany*
[b]*Institut für Organische Chemie, Universität Regensburg, Universitätsstrasse 31, D-93040 Regensburg, Germany*
[c]*Product Development, PO Box 1, Mallinckrodt Baker B.V., Rijsterborgherweg 20, NL-7400 AA Deventer, Netherlands*

Received 12 May 1997; received in revised form 1 August 1997; accepted 6 August 1997

Abstract

We present a high-performance liquid chromatography (HPLC) and a capillary zone electrophoresis (CZE) method for the chiral separation of 3-phenyl-3-(2-pyridyl)propylamines, -guanidines and -guanidine-N-carboxylic acid esters. The N-alkoxycarbonylguanidines were resolved into enantiomers on a Chiralpak AD column with resolutions ≥2.0. The separation of chloro-substituted 3-phenyl-3-(2-pyridyl)propylamines was performed on a Cyclobond I column and a RP18 column, dynamically coated with β-cyclodextrin (CD). The analytical resolution of all compounds was achieved by CZE using α-, β- or γ-CD as chiral selectors. After determination of the best suited CD, buffer pH, CD concentration and capillary temperature were optimized for each individual analyte, resulting in resolutions ≥1.2. © 1998 Elsevier Science B.V.

Keywords: Enantiomer separation; Phenylpyridylpropylamines; Arpromidine; Guanidines; Histamine agonists

1. Introduction

Arpromidine and related imidazolylpropyl-guanidines [1] are highly potent histamine H_2 receptor agonists achieving up to 150-times histamine's potency in vitro (isolated guinea pig right atrium). Moreover, in preclinical in vivo investigations these substances, in particular the difluorinated arpromidine analogues, proved to be superior to the H_2 agonist impromidine [2] (Fig. 1).

Unlike impromidine, the arpromidine-type compounds are chiral due to the phenyl(pyridyl)propyl portion which is chemically derived from the pheniramine series of histamine H_1 receptor antagonists (cf. Fig. 1). The stereochemical properties of pheniramine-type tertiary amines and the biological effects of their enantiomers are well documented (for a review see Ref. [3]). By contrast, in the arpromidine-type H_2 agonist series only the (*S*)- and the (*R*)-enantiomer of the *p*-chloro analogue have been prepared so far [4]. The determination of the

*Corresponding author.

[1]Dedicated to Professor Dr. Gerhard Franz on the occasion of his 60th birthday.

0021-9673/98/$19.00
PII S0021-9673(97)00848-0

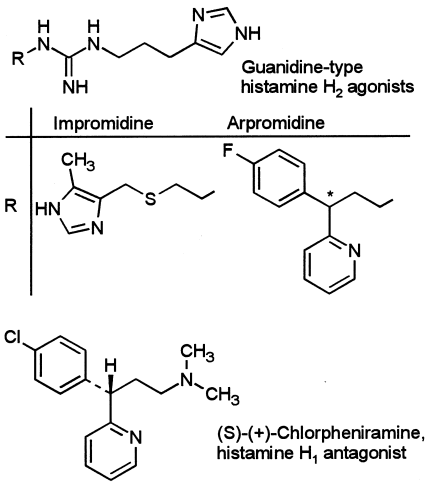

Fig. 1. Chemical structures of selected histamine H_2 receptor agonists and of the H_1 antihistaminic (*S*)-(+)-chlorpheniramine.

stereochemical purity proved to be difficult, mainly because of the strong basicity of the guanidino group and the high polarity of the guanidinium salts, respectively. Methods for the chiral separation of such compounds are of general interest as guanidino or amidino groups are found in many newly developed classes of drugs, for example as arginine-mimicking substructures in inhibitors/antagonists of thrombin, factor Xa, fibrinogen or neuropeptide Y. Here we present the results of our work on the chiral separation of arpromidine-type guanidines 11–14, of pheniramine-like primary amines 1–4 [5] required as building blocks and of alkyl guanidine-N-carboxylates 5–10 [6,7] which are useful synthetic intermediates for the preparation of guanidines 11–14 and orally active H_2 agonist prodrugs as well [8]. For structures see Table 1.

Table 1
Structures of the investigated amines 1–4, alkyl guanidine-N-carboxylates 5–10 and arpromidine-type guanidines 11–14

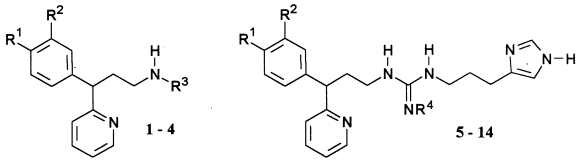

Compound	R^1	R^2	R^3	R^4
1	F	H	H	–
2	F	F	H	–
3	Cl	H	H	–
4	Cl	Cl	H	–
5	F	H	–	CO_2Et
6	F	H	–	CO_2tBu
7	F	F	–	CO_2Et
8	F	F	–	CO_2tBu
9	Cl	H	–	CO_2Et
10	Cl	Cl	–	CO_2Et
11[a]	F	H	–	H
12	F	F	–	H
13	Cl	H	–	H
14	Cl	Cl	–	H

[a] Arpromidine.

2. Experimental

2.1. Reagents and samples

The chiral selectors α- and β-cyclodextrin (CD) were purchased from Fluka (Neu-Ulm, Germany) whereas γ-CD was a kind gift from Wacker Chemie (Munich, Germany). Urea (electrophoresis reagent) and diethylamine were obtained from Sigma (Deisenhofen, Germany). Water was purified by a Milli-Q system (Millipore, Eschborn, Germany). All other reagents and solvents were of analytical or HPLC grade.

The amines 1–4, esters 5–10 and guanidines 11–14 were synthesized as previously described [1,5,6,8]. In brief, the guanidine-N-carboxylic acid esters 5–10 were prepared from the primary amines 1–4 and 3-(imidazol-4-yl)propanamine, respectively, by consecutive aminolysis of the pertinent diphenoxymethylenecarbamic acid esters. The hydrolysis of ethyl esters to guanidines was performed by refluxing with 20% hydrochloric acid for 7–10 h, whereas the *tert*.-butoxycarbonyl group was cleaved with 1 *M* HCl at ambient temperature.

Except for the 4-chloro series, i.e., compounds 3, 9 and 13, and the amine 4 only the racemates were available. Amine 3 was resolved via diasteromeric salts with *o*-nitrotartranilic acid according to a described procedure [9]. Seed crystals of both enantiomers were kindly provided by Dr. A.J. Beld, University of Nijmegen, Netherlands. The (*S*)- and (*R*)-esters 9 and (*S*)- and (*R*)-guanidines 13 were synthesized from the chiral precursors by analogy

with the racemates [1,6]. Optical rotation was measured in ethanol according to a routine procedure at 589.3 nm and 20°C. The preparation of the amine (*R*)-4 and the crystal structure of its precursor (*R*)-4-(3,4-dichlorophenyl)-4-(2-pyridyl)butanoic acid will be reported in detail elsewhere.

The enantiomeric purities of the synthesized (*R*)- and (*S*)-antipodes of the 4-chloro series (compounds 3, 9 and 13) were measured with the optimized capillary zone electrophoresis (CZE) method (cf. Table 5). Enantiomeric excess (% ee) was calculated from the peak areas, which were corrected for migration time to pay attention to the different residence times of the enantiomeric analytes in the detector window [10]. The differences in UV absorbance of the diastereomeric inclusion complexes formed with the enantiomers were negligibly small. The following % ee values were determined: 96.7 for *R*-(−)-3, 95.2 for *S*-(+)-3, 91.2 for *R*-(−)-9, 92.9 for *S*-(+)-9, 90.8 for *R*-(+)-13 and 92.4 for *S*-(−)-13.

For high-performance liquid chromatography (HPLC), the analytes were dissolved in mobile phase. For CZE measurements stock solutions were prepared. For this purpose, the amines 1–4 and the esters 5–10 were dissolved in methanol, whereas the guanidines 11–14 were dissolved in water. These stock solutions had an analyte concentration in the range from 1.3 to 33 m*M*, and were stored at −20°C. The final analyte concentration of usually 500 μ*M* was obtained by mixing the stock solutions with background electrolyte (dilute running buffer without cyclodextrin), generally yielding a sodium concentration of 15 m*M* and an urea concentration of 0.6 *M* in the sample.

2.2. Chromatography

The chromatographic systems referred to in the Tables 2–4 consisted of the following components:

System A (referred to in Table 2): the HPLC system consisted of a Model LC-250 pump (Perkin-Elmer, Norwalk, CT, USA), a 7125 injector (Rheodyne, Cotati, CA, USA) with a 20-μl sample loop and a Model LC-290 UV–Vis variable-wavelength spectrophotometer (Perkin-Elmer). Data from this system were collected using a Model BD 111 flatbed recorder (Kipp and Zonen, Delft, Netherlands). A mistral column thermostat (Spark Holland, Emmen, Netherlands) was used to obtain reproducible operating conditions.

System B (referred to in Tables 2 and 4): SP 8700 solvent delivery system (Spectra-Physics, Darmstadt, Germany), Rheodyne 7125 sample injector (injection volume 1, 5 or 10 μl), variable UV detector Model 1050 (Hewlett-Packard, Böblingen, Germany), 254 nm, connected to a SP4000 integrating system (Spectra-Physics).

System C (referred to in Tables 3 and 4): pump Model 2150 (LKB, Freiburg, Germany), Rheodyne 7125 sample injector, Model 655A variable-wavelength UV detector (Merck, Darmstadt, Germany), set to 254 nm, Model D2000 Chromato-Integrator (Merck–Hitachi, Darmstadt, Germany) and a Bio-Rad instrument interface (Bio-Rad, Munich, Germany), respectively. The columns were thermostatted with a KT6 CZ cryostat (MLW-Electronic, Berlin, Germany). The sign of the optical rotation of the separated enantiomers was measured online with a Shodex Model OR-1 optical rotation detector (Techlab, Erkerode, Germany) at 780 nm. For these measurements, analyte solutions of 3.18–5.15 mg/ml were used. The injection volume was 20 μl.

The following HPLC columns were used (the underlined acronyms and abbreviations are used in Tables 2–4):

Chiralpak AD [amylose tris(3,5-dimethylphenylcarbamate), 10 μm], Chiralcel OD (10 μm), Chiralcel OD-H (5 μm), Chiralcel OD-R [10 μm, all cellulose tris(3,5-dimethylphenylcarbamate)], Chiralcel OB-H (cellulose tribenzoate, 5 μm), Chiralcel OJ [cellulose tris(*p*-methylbenzoate), 10 μm] and Chiralcel OF [cellulose tris(*p*-chlorophenylcarbamate), 10 μm], all 250×4.6 mm, manufactured by Daicel (Tokyo, Japan); Chiralpak AD (250×4.6 mm, 10 μm, Baker, Gross-Gerau, Germany), protected by a corresponding pre-column (50×4.6 mm).

(*R*)-N-3,5-Dinitrobenzoylphenylglycin (DNBPG) covalent, (5 μm, 250×4.6 mm), purchased from Mallinckrodt Baker (Griesheim, Germany); triacetylcellulose (TAC, 10 μm, 250×10.0 mm), ChiraSpher (CS, 5 μm, 250×4.0 mm) and ChiraDex GAMMA (CDG, 5 μm, 250×4.0 mm), all distributed by Merck; Cyclobond I (CBI, 5 μm, 250×4.6 mm) distributed by ICT (Bad Homburg v.d.H., Germany).

Table 2
Experiments for enantiomeric separation of the analytes 1–13 on various chiral HPLC colums (cf. Section 2.2)

Compound	Amount (μg)	System	Column	Eluent	Temperature (°C)	t_{r1} (min)	t_{r2} (min)	k'_1	k'_2	α	R_s
1	2.5	A	AD	B	30	12.4[d]	12.4[d]	1.06	1.06	1.00	0
2	2.5	A	AD	B	30	11.5[d]	11.5[d]	0.82	0.82	1.00	0
4	4.2	A	AD	B	30	12.8[d]	14.5[d]	1.11	1.39	1.25	0.6[f]
4	4.2	A	OD	A[a]	25	10.75	10.75	2.52	2.52	1.00	0
5	2.6	A	AD	B	30	14.93	16.99	1.45	1.79	1.23	2.2
5	2.4	A	OD	A[a]	25	11.82	12.21	3.04	3.17	1.04	≤0.5
7	2.4	A	AD	B	30	13.64	14.76	1.35	1.54	1.14	1.3
7	2.4	A	OD	A[a]	25	12.82	12.82	3.38	3.38	1.00	0
10	2.6	A	AD	B	30	15.60	20.02	1.52	2.24	1.47	3.9
10	2.5	A	OD	A	25	26.96	26.96	3.41	3.41	1.00	0
12	2.5	A	AD	B	30	>19[e]	>19[e]	n.d.	n.d.	n.d.	n.d.
12	2.6	A	AD	D[a]	25	5.05	5.05	0.72	0.72	1.00	0
12	1.5	A	OD	D[a]	25	5.46	5.46	1.03	1.03	1.00	0
12	1.3	A	OJ	A[a]	25	7.63	7.63	1.33	1.33	1.00	0
12	1.3	A	OJ	C	25	14.3	14.3	1.39	1.39	1.00	0
12	1.5	A	OD-R	I	25	10.97	10.97	1.06	1.06	1.00	0
12	2.6	A	OD-H	D	40	11.14	11.14	0.68	0.68	1.00	0
12	1.3	A	OB-H	D	25	13.64	13.64	2.04	2.04	1.00	0
12	1.5	A	OF	D	40	13.74	13.74	1.07	1.07	1.00	0
13	5.1	B	DNBPG	F[b]	25	2.88[d]	2.88[d]	3.0	3.0	1.00	0
13	25.7	B	TAC	H[c]	25	>70[e]	>70[e]	n.d.	n.d.	n.d.	n.d.
13	22.2	B	CS	G[a]	25	6.32	6.32	1.19	1.19	1.00	0
13	2.5	A	AD	B	30	>23[e]	>23[e]	n.d.	n.d.	n.d.	n.d.
13	1.25	A	AD	D[a]	25	31.5[d]	31.5[d]	9.43	9.43	1.00	0
13	1.25	A	OD	E	25	21.1	21.1	2.81	2.81	1.00	0
13	1.25	A	OJ	A[a]	25	~30[d]	~30[d]	~9	~9	1.00	0
13	1.25	A	OJ	C	25	25.3	25.3	3.45	3.45	1.00	0
13	1.25	A	OD-R	I	25	5.32	5.32	~0	~0	~1.00	0
13	1.25	A	OD-H	C	25	26.2[d]	26.2[d]	2.91	2.91	1.00	0
13	1.25	A	OD-H	D	25	43.2[d]	43.2[d]	5.22	5.22	1.00	0
13	1.25	A	OB-H	D	25	~32[d]	~32[d]	6.2	6.2	1.00	0

Mobile phases: A, B: *n*-hexane–ethanol–diethylamine: A=(90:10:0.1); B=(80:20:0.1); C: *n*-hexane–ethanol–trifluoroacetic acid (TFA) (90:10:0.1); D, E: *n*-hexane–2-propanol–TFA: D=(90:10:0.1); E=(80:20:0.1); F: *n*-hexane–2-propanol–methanol (50:25:25, flow 1.5 ml/min); G: *tert*.-butyl methyl ether–tetrahydrofurane–methanol (48:25:27, flow 1.0 ml/min); H: ethanol–water (96:4, flow 2.0 ml/min); I: acetonitrile–0.5 *M* $NaClO_4$ (40:60, pH 2.0); all ratios are v/v. The flow-rate was 0.5 ml/min, unless otherwise indicated. Exceptions: [a] 1.0 ml/min; [b] 1.5 ml/min; [c] 2.0 ml/min.
Remarks: n.d.: not determinable; [d] elution as broad peak; [e] no elution observed; [f] value estimated because of severe peak distortion.

In addition, three reversed-phase columns were coated dynamically with β-CD or γ-CD by pumping eluent K or L for 30 min (flow 1.0 ml/min) through a LiChrospher 100 RP-18 endcapped (250×4.0 mm, 5 μm, Merck), resulting in R18a, through a LiChrospher Select B (250×4.0 mm, 5 μm, Merck), resulting in R8S, or through a LiChrosorb ODS (250×4 mm, 7 μm, Merck), protected by a corre-

Table 3
Optimized chromatographic conditions and parameters for the chiral separation of the esters 5–10 on a Chiralpak AD column with system C (cf. Section 2.2)

Compound	Amount (μg)	*n*-Hexane (%)	EtOH (%)	t_{r1} (min)	t_{r2} (min)	k'_1	k'_2	R_s	α
5	8.0	88	12	30.88	35.76	3.27	3.94	3.1	1.21
6	5.0	90	10	20.70	23.71	1.83	2.24	3.1	1.22
7	5.0	90	10	39.29	43.16	4.32	4.85	2.0	1.12
8	6.4	92	8	28.58	31.84	2.61	3.02	2.4	1.16
9	8.0	85	15	24.93	33.22	2.42	3.56	5.4	1.47
10	11.4	85	15	23.06	27.12	2.10	2.64	3.4	1.26

The mobile phases consisted of mixtures of *n*-hexane and ethanol of varying compositions, to which 0.1% (v/v) diethylamine was added.

sponding pre-column (30×4 mm), resulting in R18b (Table 4).

Helium degassed mixtures of two or three solvents were used isocratically with regard to the special nature of the chiral columns. Buffers were filtered using membrane filters (0.65 μm, Millipore). The detailed composition, pH and temperature of the mobile phases are listed in the footnotes of Table 2. The flow-rate was 0.5 ml/min unless otherwise indicated.

2.3. Capillary electrophoresis

CZE was performed with a Biofocus 3000 capillary electrophoresis system (Bio-Rad). Chiral separations were carried out in a 75 (effective length 70.4 cm)×50 μm I.D. fused-silica capillary (Microquarz, Gesellschaft für Quarzglaskomponenten, Munich, Germany). The voltage (positive mode) was set at 20 kV, resulting in a field strength of 266.7 V/cm. In order to obtain reproducible operating conditions with respect to the capillary surface, before hydrodynamical injection of the samples at a constant pressure–time integral of 20 p.s.i.·s (1 p.s.i.= 6894.76 Pa), the capillary was flushed with 0.1 *M* NaOH for 5 min, with water for 2 min and finally with running buffer for 10 min. The UV detector was set to 210 nm.

For the preparation of the running buffers 125 m*M* $NaH_2PO_4 \cdot H_2O$ and 5 *M* urea were dissolved in

Table 4
Experiments for chiral HPLC separations on β- and γ-CD coated columns at 25°C (systems B and C, cf. Section 2.2)

Compound	Column	Eluent	t_{r1} (min)	t_{r2} (min)	k'_1	k'_2	R_s	α
13	R8S	K1[a]	33.0	33.0	8.07	8.07	0	1.0
13	R18a	K1	51.3	51.3	19.7	19.7	0	1.0
13	R18a	K2	148.6[b]	148.6[b]	63	63	0	1.0
13	R18a	K3	>166	>166	>70	>70	n.d.	n.d.
3	R18b	L	39.0	40.3	15.0	15.5	n.d.	1.03
4	R18b	L	72.5	76.6	26.8	28.3	0.9	1.06
3	CBI	M	13.0	13.8	3.44	3.68	0.9	1.07
4	CBI	M	27.4	30.0	8.20	9.08	1.3	1.11
13	CDG	N	7.9	7.9	n.d.	n.d.	0	1.0
13	CDG	O	53.0	53.0	n.d.	n.d.	0	1.0
13	CDG	P	25.1[c]	25.1[c]	n.d.	n.d.	0	1.0

Mobile phases: K: methanol–0.01 *M* KH_2PO_4/H_3PO_4 [20:80, v/v, 7.40 m*M* γ-CD, pH 2.6 (K1) 3.8 (K2) 7.0 (K3)]; L: acetonitrile–1% (w/v) triethylammonium acetate pH 4.6 (10:90, v/v), 2 g/100 ml eluent β-CD); M: acetonitrile–1% (w/v) triethylammonium acetate pH 4.6 (10:90, v/v); N: methanol–0.01 *M* KH_2PO_4/K_2HPO_4 (50:50, pH 7.0); O: 0.01 *M* KH_2PO_4/K_2HPO_4 (pH 7.0); P: 0.02 *M* KH_2PO_4/K_2HPO_4 (2.0 *M* urea, pH 7.0). Flow 1.0 ml/min, unless otherwise indicated.
Remarks: n.d.: not determinable; [a] flow: 0.7 ml/min; [b] strong tailing; [c] neither reduction of flow (0.66 ml/min) nor higher urea concentrations (up to 5 *M*) could produce any resolution.

water, and the pH was adjusted by adding appropriate amounts of 85% H_3PO_4 and NaOH (conc.), respectively. The CDs were dissolved in these sodium phosphate buffers. CD concentrations were calculated as $c^* = n(\text{CD})/v(\text{solvent})$ (mM). The high urea concentration was necessary to increase the water solubility of the CDs, in particular of β-CD. Urea slowly decomposes in water to CO_2 and NH_3. To preclude changes of the buffer pH, the buffers were made freshly every few days. To reach the required high concentrations of α- and β-CD in the sodium phosphate buffers, the solutions were sonicated and subsequently carefully heated on a water bath. For dissolving γ-CD at the required high concentrations, sonication alone was sufficient. Because of the high viscosity of the running buffers, these solutions were used without final filtration.

3. Results and discussion

3.1. HPLC

3.1.1. Experiments with various chiral stationary phases

Our attempts to find a column suitable for the separation of arpromidine-type guanidines failed. The results of our screening experiments testing numerous chiral materials for representative analytes are summarized in Table 2.

The strong basic nature especially of the guanidino group (compounds 12 and 13) caused intense adsorption on Chiralpak AD, which could not be overcome even by addition of an amine modifier. Amines 1 and 2 were eluted, but only as broad, unresolved peaks. However, compound 4 showed some enantiomeric separation, favoured by its chlorine substitution. But heavy peak distortion, caused by strong adsorption of the basic amino group, prevented good resolution in spite of sufficient selectivity. Indeed, substitution of the NH_2 group in 4 by a COOH moiety led to almost complete chiral separation (data not shown). On the other hand, the enantiomeric ion pairs, generated with 1–4 in acidic eluents, could not be separated at all.

Additionally, neither Pirkle-type I columns like DNBPG nor protein phases (i.e., α-AGP, data not shown) proved to be suitable.

However, these studies revealed that the resolution of racemic alkyl guanidine-N-carboxylic acid esters is feasible on a Chiralpak AD column. As already discussed for the amines, dichloro substituted enantiomers are separated more easily than the corresponding unsubstituted or fluorinated compounds.

Interestingly, Chiralcel OD [cellulose tris(3,5-dimethylphenylcarbamate)] failed in enantiomeric separation of the guanidine-N-carboxylates and the amine 4 (cf. Table 2). On the one hand none of all the other cellulose based chiral phases were satisfactory. On the other hand it is well known, that cellulose and amylose derivatives do rather complement than substitute each other with regard to their applications. Polysaccharide based stationary phases show different helical higher-order structures, which often are more efficient for chiral resolution than variations of the nature of the substituents [11]. In this context CDs become interesting compounds for the HPLC separation of the title compounds (cf. Section 3.1.3).

3.1.2. Separations on amylose-tris(3,5-dimethylphenylcarbamate) material

The chiral separation of the racemic esters (5–10) was achieved on Chiralpak AD with system C. Column temperature and flow-rate had only a minimal effect on peak resolution. Therefore, separations were carried out at 40°C with a flow-rate of 0.5 ml/min to shorten analysis times. Due to strict limitations with respect to the use of Chiralpak AD compatible solvents, optimization procedures were focused on the variation of the ethanol content of the mobile phase. The compositions of the mobile phases, which yielded baseline separation, and the resulting chromatographic parameters are given in Table 3. As is evident from Table 3, all esters were separated with selectivities (α) of at least 1.21 and minimal resolutions (R_s) of 2.0. A representative chromatogram of an optimized separation is shown in Fig. 2. The direction of the optical rotation of the separated enantiomers was determined online with an optical rotation detector at a wavelength of 780 nm. The order of elution was the same for all esters: the laevorotatory enantiomers were detected first, followed by the dextrorotatory enantiomers. The sign of the optical rotation of the enantiomers of the ester 9 was the same at 780 nm (in mobile phase) and at

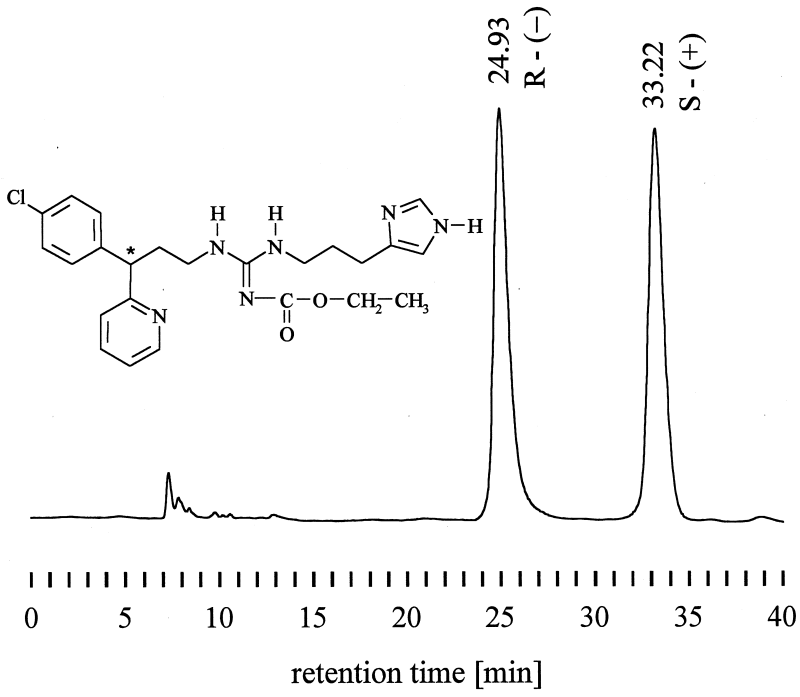

Fig. 2. Representative chromatogram of the chiral separation of the ester 9 on a Chiralpak AD column. Injection volume: 20 μl; analyte concentration: 0.4 mg in 1 ml mobile phase; column temperature: 40°C; mobile phase: *n*-hexane–ethanol–diethylamine (85:15:0.1); flow: 0.5 ml/min.

589.3 nm (in ethanol), the standard wavelength used in conventional polarimetric measurements. Fig. 3 shows the UV and the optical rotation signal, obtained after chiral separation of the ester 6.

3.1.3. Experiments with β- and γ-CD as stationary phase

For many years CDs have been widely used for performing HPLC chiral separations, both as chiral eluent modifiers and covalently bound to the stationary phases [12]. Piperaki et al. [13] were successful in separating fluoxetine and norfluoxetine, amine compounds similar to 1–4, by CZE and HPLC (with β-CD both as eluent modifier and covalently bound stationary phase). As γ-CD proved to be the best suited additive for CZE enantiomeric separation of the guanidine 13 (cf. Section 3.2), we ''coated'' two different columns, a LiChrospher Select B (a C_8 material especially modified for basic analytes; designated R8S in Table 4), and a LiChrospher 100 RP18 endcapped (designated R18a) with potassium phosphate buffers containing 7.40 m*M* γ-CD. Despite the high CD concentration in the eluent separation of the enantiomers failed with both columns (cf. Table 4) regardless of the pH of the mobile phase (pH is known to strongly influence CD induced chiral separations [14]). There was also no change in retention time of 13 in the presence or absence of CD. This observation suggests that the concentration of analyte–CD complexes must have been very low. Therefore, it is not surprising that ChiraDex GAMMA also failed in the chiral resolution of 13.

On the contrary, amines 3 and 4 could be successfully separated on a β-CD modified silica gel (Cyclobond I) after optimization of the buffer pH (variation between 3.6 and 5.1), buffer concentration (0.2% and 1% at pH 4.6) and the organic solvent (methanol and acetonitrile) (cf. Table 4). Under identical conditions, slightly lower resolutions were achieved on a Lichrosorb ODS column (designated R18b), dynamically coated with 20 g β-CD per liter

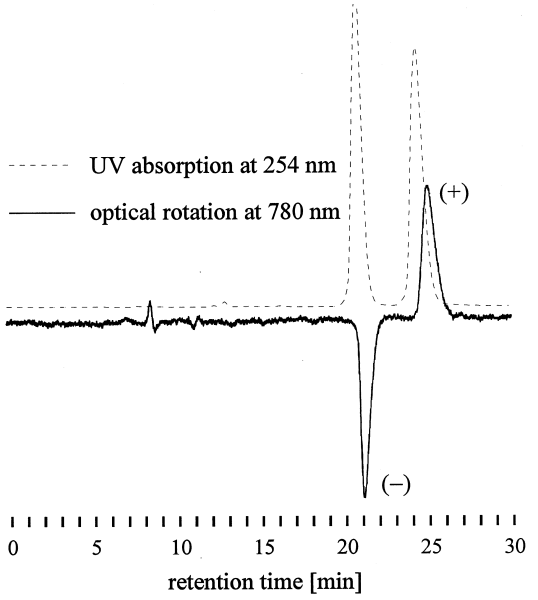

Fig. 3. UV and optical rotation signal for the chiral separation of the ester 6 on a Chiralpak AD column. Injection volume: 20 μl; analyte concentration: 4.35 mg in 1 ml mobile phase; column temperature: 40°C; mobile phase: *n*-hexane–ethanol–diethylamine (90:10:0.1); flow: 0.5 ml/min.

of eluent (cf. Table 4). However, resolution of compounds 1, 2, 9 and 13 failed with both chromatographic systems.

3.2. Capillary zone electrophoresis

3.2.1. Inclusion complexation with CDs

The successful chiral separation of the H_1 antihistaminic chlorpheniramine, which is structurally very similar to the primary amine 3 (chlorpheniramine has two additional methyl groups at the amine nitrogen, cf. Fig. 1), with CZE using β-CD as chiral selector [15], prompted us to apply this technique to the arpromidine-type guanidines and to their ester and amine precursors. Due to the phenyl and pyridyl groups of these compounds, the formation of host–guest complexes with CDs, a prerequisite for chiral resolution, was most likely. Therefore, we tested the commercially available natural oligosaccharides α-, β- and γ-CD for the chiral separation of compounds 1–14. Due to the high concentrations of urea and the chiral selectors in the running buffers, resulting in elevated viscosities, the migration slowed down providing sufficient time for the separation of the CD complexed optical antipodes. For each analyte, optimization of the CZE method was performed according to Fig. 4.

3.2.2. Effect of CD ring size

A prerequisite for inclusion complexation is a good fit of the analytes into the cavity of the CD. Therefore, the appropriate chiral selector with the correct internal diameter had to be found with respect to the molecular dimension and the shape of each individual analyte. For this purpose, 100 m*M* α-CD, 100 m*M* β-CD and 100 m*M* γ-CD were added separately to a background electrolyte (pH 2.5), and the effect of the ring size on the resolution

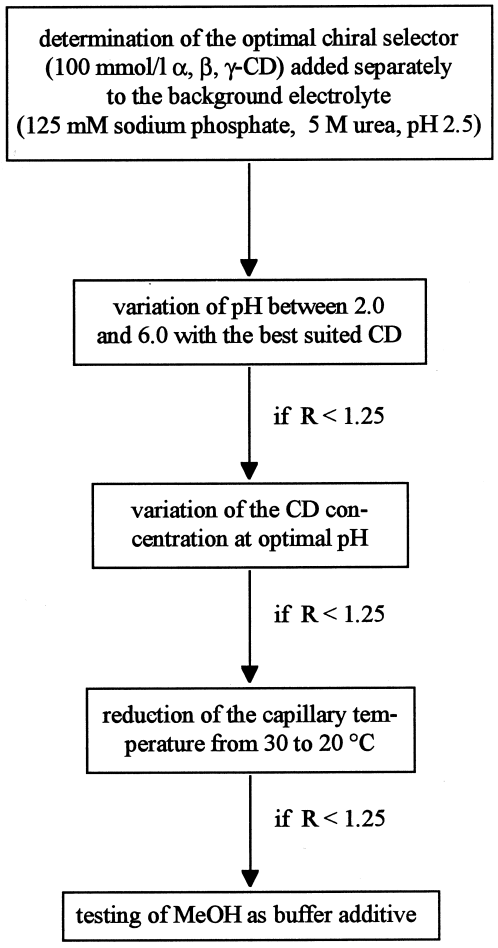

Fig. 4. Optimization procedure for CZE separation. *R*= Resolution.

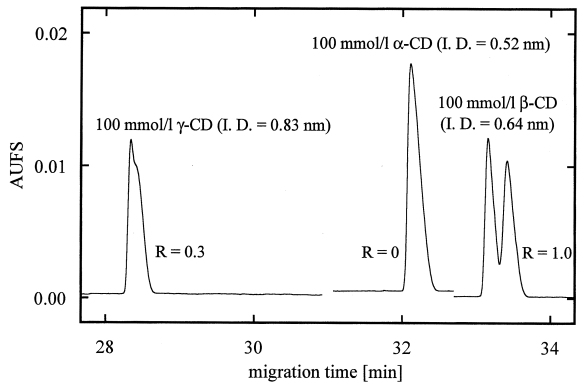

Fig. 5. Effect of the ring size of the CD on the separation of the guanidine 11. Analyte concentration: 530 μ*M* in 1:5 diluted background electrolyte; capillary temperature: 30°C; running buffer: 100 m*M* CD in 5 *M* urea and 125 m*M* sodium phosphate buffer, pH 2.5.

of the enantiomers of each analyte was measured. Fig. 5 shows the electropherograms, which were obtained for the guanidine 11. As can be seen from Fig. 5, the addition of α-CD failed to separate the racemic mixture into its enantiomers, whereas with γ-CD the optical antipodes were partly resolved. For the guanidine 11, best separation was achieved with β-CD. Moreover, it is evident from the order of the migration times, that 11 has a higher affinity to α-CD (relatively small complex) than to γ-CD (bulky complex), although the differences in retardation of the enantiomers of compound 11 are greater with γ-CD than with α-CD. The differences of apparent mobilities were highest with β-CD as chiral selector.

3.2.3. Optimization of background electrolyte pH

In chiral recognition by CDs hydrophobic and electrostatic interactions as well as the formation of hydrogen bonds are usually involved [16], all factors, which are strongly influenced by pH. As all of the compounds 1–14 contain basic groups, acidic background electrolytes were used.

To find the optimal hydronium ion concentration for the chiral separation of each racemate, the pH of the different background electrolytes was varied between 2.0 and 6.0. As can be seen from Table 5, for all analytes best resolutions were obtained within the pH range from 2.0 to 3.0. Because under the strongly acidic conditions used, the electroosmotic flow (EOF) is completely suppressed, the residence time of the analytes in the capillary was also sufficient for the separation of those enantiomers, characterized by minimal differences in migration. Thus, the suppression of the EOF (EOF always has a detrimental effect on the resolution of cationic enantiomers [17]) by the use of dynamically or covalently coated capillaries was unnecessary. Fig. 6 shows the pH dependence of the enantiomeric separation of the ester 9. It is obvious from Fig. 6 that differential retardation of the optical antipodes was strongly influenced by pH, being maximal at pH 2.0. Electrophoretic mobility of the enantiomers depends

Table 5
Optimized electrophoretic conditions and parameters for the chiral separation of all analytes 1–14

Compound	Chiral selector	Buffer-pH	Capillary temperature (°C)	t_{m1} (min)	t_{m2} (min)	R_s
1	100 m*M* α-CD	2.0	30	34.81	35.50	2.7
2	175 m*M* γ-CD	2.0	30	44.81	45.59	2.7
3	100 m*M* γ-CD	2.5	20	44.16	45.44	3.6
4	175 m*M* γ-CD	2.0	30	63.72	65.41	3.9
5	100 m*M* β-CD	3.0	20	43.28	43.87	1.4
6	125 m*M* β-CD	2.0	20	79.11	79.95	1.3
7	100 m*M* β-CD	3.0	20	46.72	47.34	1.2
8	250 m*M* γ-CD[a]	2.5	30	78.36	79.08	1.2
9	100 m*M* β-CD	2.0	20	61.54	62.62	2.2
10	175 m*M* γ-CD	2.0	30	66.68	67.75	2.3
11	125 m*M* β-CD	2.0	20	50.48	51.05	1.7
12	250 m*M* γ-CD	2.0	20	82.94	83.73	1.6
13	125 m*M* γ-CD	2.5	20	47.15	47.69	1.6
14	175 m*M* γ-CD	2.0	30	58.37	59.03	1.9

[a] 10% (v/v) MeOH was added to the running buffer.

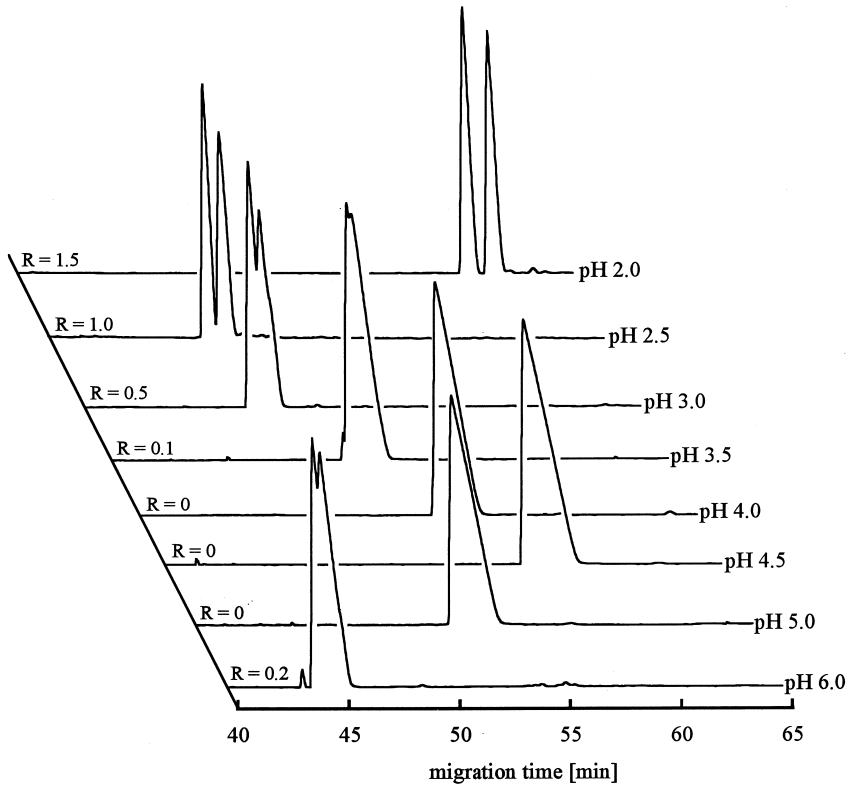

Fig. 6. Effect of buffer pH on the separation of the ester 9. Analyte concentration: 2.5 m*M* in 1:10 diluted background electrolyte, pH 4.0; capillary temperature: 20°C; running buffer: 100 m*M* β-CD in 5 *M* urea and 125 m*M* sodium phosphate buffer of various pH.

on the charge of the analyte, on the formation constants of the inclusion complex and on the EOF. Since all three factors are strongly influenced by pH, producing opposite effects in part, no trend in migration time can be seen in Fig. 6. Interestingly, for most compounds there was a large increase in migration times between pH 2.5 and 2.0. This observation can neither be explained by the different degree of protonation of the analytes (imidazole rings have pK_a values around 7, pyridine rings in pheniramine-like compounds have pK_a values around 4) nor by changes of the EOF, being already minimal at pH 2.5. It can be speculated that a change in viscosity, analyte conformation or altered interactions of the buffer components with the capillary wall might be responsible for this phenomenon.

3.2.4. Variation of the concentration of the chiral selector

The CD concentration plays an important role in the optimization procedure, as the equilibrium of complex formation is strongly influenced by this parameter.

For all analytes, for which baseline separation could not be achieved under the above described conditions, measurements with different CD concentrations were performed. The highest concentrations used were 100 m*M* for α-CD, 125 m*M* for β-CD and 250 m*M* for γ-CD. An example for the selection of the appropriate concentration of the chiral selector is given in Fig. 7, illustrating the influence of β-CD concentration on the separation of the ester 5. As can be seen from Fig. 7, mobility differences continuously increased up to a β-CD concentration of 125 m*M*. Concomitantly, a prolongation of the migration times was observed. This phenomenon can be explained by the growing buffer viscosity and a shift of the equilibrium in favour of the inclusion complexes by increasing CD concentration. At 125 m*M* of β-CD (the maximal

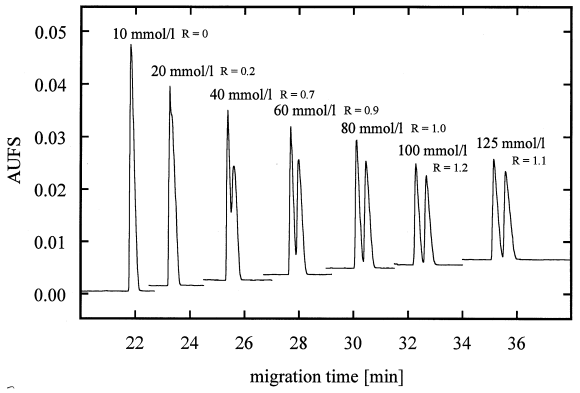

Fig. 7. Effect of β-CD concentration on the separation of the ester 5. Analyte concentration: 540 μ*M* in 1:8.3 diluted background electrolyte, pH 2.5; capillary temperature: 30°C; running buffer: β-CD of various concentration in 5 *M* urea and 125 m*M* sodium phosphate buffer, pH 3.0.

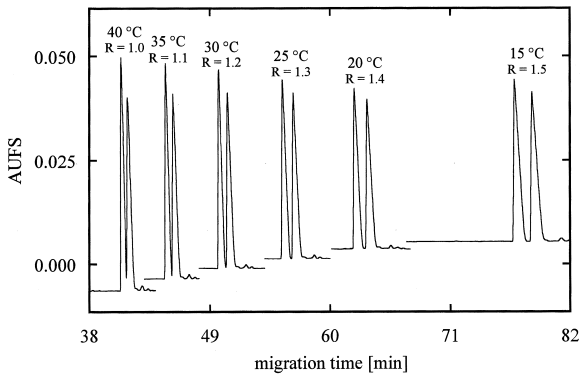

Fig. 8. Effect of capillary temperature on the chiral separation of the ester 9. Analyte concentration: 2.5 m*M* in 1:10 diluted background electrolyte; running buffer: 100 m*M* β-CD in 5 *M* urea and 125 m*M* sodium phosphate buffer, pH 2.0.

concentration tested), resolution slightly deteriorated, probably due to diffusion taking effect at long analysis times.

As can be seen from Table 5, best enantiomeric separations were obtained for all analytes at very high CD concentrations. However, to minimize both, analysis time and the risk of capillary clogging, CD concentration was only elevated until baseline separation was achieved, when γ-CD was used. This procedure seems appropriate since resolutions always increased with increasing γ-CD concentration, and no optimum was observed within the examined concentration range.

3.2.5. Effect of temperature

An elevation of the capillary temperature leads to reduced buffer viscosity and thus to an increase in electrophoretic and electroosmotic mobility. Lower temperatures prolong the residence time of the analyte in the capillary, and more time is available for separation. Generally, a decrease in temperature also results in an increase in the binding constants of the inclusion complexes [18,19] and, consequently, in a more pronounced difference in the complex formation constants of the enantiomers.

Fig. 8 shows the influence of the capillary temperature on the separation of the ester 9. Resolutions improve with declining temperature, paralleled by prolonged analysis time. Therefore, according to the flow chart, the separation of compounds 1–14 was done at 30°C, provided that resolution was sufficient (R_s>1.25) after the above described optimization procedures. If the analytes were not baseline separated at 30°C, the temperature was reduced to 20°C at the expense of analysis time.

3.2.6. Methanol as buffer additive

Because the separation of ester 8 was insufficient after the above outlined optimization procedures, methanol was tested as an organic modifier. Addition of methanol to the background electrolyte reduces electrical current, improving the efficiency of the system due to decreased Joule heating. Moreover, the addition of an organic solvent may improve selectivity, if the solvent exerts a differential influence on the complex formation constants of the two enantiomers. If, as is generally assumed, the hydrophobic portion of the analyte fits inside the hydrophobic CD cavity, the addition of methanol should reduce the affinity of the analyte for the CD, owing to better solubility of the analytes in the background electrolyte. Consequently, separation should become worse.

However, as shown in Fig. 9 for the chiral separation of compound 8, the addition of methanol improved resolution, and best results were obtained with 10% (v/v) methanol.

Although the viscosity of the buffer was increased by the addition of methanol, migration times were shortened. This phenomenon may be caused by decreased binding constants of the CD inclusion complexes due to the aforementioned competition with the buffer additive methanol.

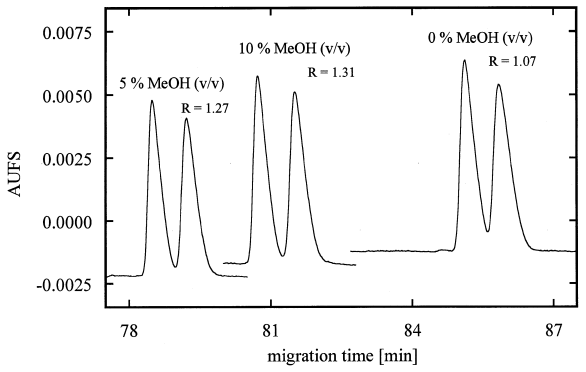

Fig. 9. Effect of the buffer additive methanol on the separation of the ester 8. Analyte concentration: 560 μ*M* in 1:8.3 diluted background electrolyte pH 6.0; capillary temperature: 30°C; running buffer: 250 m*M* γ-CD in 5 *M* urea and 125 m*M* sodium phosphate buffer, pH 2.5.

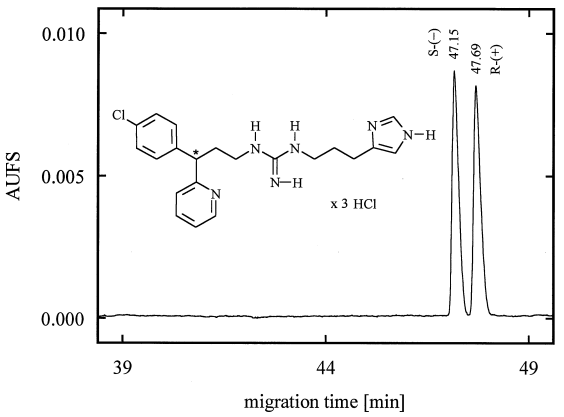

Fig. 10. Representative electropherogram of the chiral separation of the guanidine 13 using γ-CD as chiral selector. Analyte concentration: 500 μ*M* in 1:8.3 diluted background electrolyte; capillary temperature: 20°C; running buffer: 125 m*M* γ-CD in 5 *M* urea and 125 m*M* sodium phosphate buffer, pH 2.5.

3.2.7. The optimized CZE method

The optimized electrophoretic conditions and the resulting separation parameters of all analytes are summarized in Table 5. Best separations were obtained at acidic pH and relatively high CD concentrations. Table 5 also shows that there is no obvious correlation between the type of CD and the substitution pattern of the phenyl ring. This may be considered as a hint that there exist different possibilities for the formation of inclusion complexes of the CDs with the analytes. As is evident from Table 5, all racemates were separated with resolutions of at least 1.2, although analysis times were relatively long compared with the chromatographic separations (cf. Table 3). In contrast to HPLC, not only all esters but also all amines and guanidines could be separated. An example of an optimized chiral CZE separation is shown in Fig. 10.

By collecting the fractions of the chromatographically resolved esters, it was possible to isolate the individual ester enantiomers and to inject them into the CZE system. This enabled us to determine the order of migration of the esters, which was inverse to HPLC: i.e., the electrophoretic mobilities of the dextrorotatory enantiomers were higher than the mobilities of the laevorotatory enantiomers. For the 4-chloro series (compounds 3, 9 and 13) as well as for amine 4 the (*S*)-configurated enantiomers migrated faster than the respective (*R*)-compounds.

3.2.8. Considerations on the mechanism of separation

Rawjee et al. [20] published a theoretical model, describing the effects of pH and CD concentration on the chiral separation of weak bases. There are three fundamentally different types of enantiomeric separations, depending on the interacting form of the enantiomers (only uncharged, only ionic, or both) with the CD. Separation selectivity increases with increasing pH only if differential interactions of the non-ionic forms of the two enantiomers with the chiral selector are involved in separation. On the contrary, improved separation at low pH values indicates, that the distinct interactions of the ionic forms play a role in separation. Since the compounds 1–14 were separated best at low pH, it seems very likely, that the differential interaction of protonated pyridyl rings (pK_a of the pyridine ring is approx. 4) of the analytes contributes to chiral CZE separation.

In a simple mathematical model Wren and Rowe (1992) [21] showed that there is an optimum CD concentration, depending on the complex formation constants of the two enantiomers. The greater the affinity of the analytes for the chiral selector, the lower is the optimum CD concentration. This statement is valid under the assumption, that the diastereomeric inclusion complexes of the two enantiomers with the CD have in first approximation

identical electrophoretic mobilities. Separation is achieved, if the enantiomers have different affinities for the chiral selector and the electrophoretic mobilities of the free and complexed enantiomers are different.

Although the effect of organic solvents as buffer additives is difficult to predict, Wren and Rowe [22] deduced from their aforementioned mathematical model that the effect of an organic modifier on separation mainly depends on CD concentration: when the CD concentration is above the optimum value, the addition of methanol enhances the mobility differences of the enantiomers. On the contrary, if the CD concentration is at or below the optimum value, the addition of methanol reduces resolution. These predictions were made under the assumption, that methanol reduces the size of the equilibrium constants of the two enantiomers by the same percentage.

In our CZE experiments with the guanidines 11–14, the esters 5–10 and the amines 1–4 no concentration optimum of the chiral selector with respect to the differences in migration was observed (see Section 3.2.4), and the addition of methanol improved separation of the ester 8, although the γ-CD concentration was below an optimum value (cf. Section 3.2.6). In our opinion, the experimental results can be explained by the reduction of Joule heating and analyte adsorption to the capillary due to the organic modifier and/or by a differential influence of methanol on the binding constants of the two enantiomers.

Engelhardt et al. [23] proposed at least two different separation mechanisms, based on the observation that the order of elution of dansylated D,L-phenylalanine is reversed by increasing concentrations of hydroxypropylated β-CD. At low CD concentrations the separation depends on differences in the complex formation constants of the two enantiomers, whereas at high CD concentrations the separation results from the differences in the mobilities of the diastereomeric inclusion complexes formed by the enantiomers with CD. However, in our studies such an inversion did not occur.

Since optimized enantiomeric separations of the compounds 1–14 were performed at very high CD concentrations, most likely the different physical properties of the diastereomeric complexes were responsible for resolution. This would mean, that the models of Wren and Rowe [21,22] are invalid for the separation of these compounds.

4. Conclusions

We developed HPLC methods for the chiral separation of arpromidine-like alkoxycarbonylguanidines using a Chiralpak AD column and for the resolution of chloro-substituted 3-phenyl-3-(2-pyridyl)propylamines on a Cyclobond I column as well as on a RP18 column, dynamically coated with β-CD. These methods will be useful not only for various analytical purposes but also for the isolation of enantiomeric compounds for pharmacological tests as well as for the preparation of seed crystals. The analytical resolution of guanidines, esters, and amines was achieved by CZE using α-, β- or γ-CD as chiral selectors. This powerful and economical technique is useful to determine enantiomeric purities and may be valuable in pharmacokinetic and metabolic investigations.

Acknowledgements

The authors are grateful to Ms. Susanne Bollwein for technical support, to Dr. A.J. Beld for seed crystals of (+)- and (−)-3 with L- and D-*o*-nitrotartranilic acid, to Wacker Chemie for kindly providing the γ-CD, to Techlab for providing the OR-1 chiral detector, and to the Fonds der Chemischen Industrie for a grant.

References

[1] A. Buschauer, J. Med. Chem. 32 (1989) 1963.
[2] S.B. Felix, A. Buschauer, G. Baumann, Eur. J. Clin. Invest. 25(Suppl. 1) (1995) 42.
[3] C.R. Ganellin, in J.-C. Schwartz, H.L. Haas (Editors), The Histamine Receptor (Receptor Biochemistry and Methodology, Vol. 16), Wiley-Liss, New York, 1992, pp. 1–56.
[4] A. Buschauer, G. Baumann, Agents Actions, Suppl. 33 (1991) 231.
[5] A. Buschauer, Arch. Pharm. (Weinheim) 322 (1989) 165.

[6] P. Mörsdorf, H. Schickaneder, V. Pfahlert, H. Engler, A. Buschauer, W. Schunack, S. African Pat. ZA 88 01,271 (cf. Eur. Pat. Appl. EP 0 302 164); Chem. Abstr., 111 (1988) 134154x (1989).
[7] P. Mörsdorf, H. Engler, H. Schickaneder, A. Buschauer, W. Schunack, G. Baumann, Drugs Fut. 15 (1990) 919.
[8] A. Schuster, G. Bernhardt, A. Buschauer, Eur. J. Pharm. Sci. 5 (1997) 79.
[9] A.J. Beld, Thesis, University of Nijmegen, Nijmegen, Netherlands, 1980.
[10] K.D. Altria, Chromatographia 35 (1993) 177.
[11] E. Yashima, Y. Okamoto, Bull. Chem. Soc. Jpn. 68 (1995) 3289.
[12] A.M. Krstulović (Editor), Chiral Separations by HPLC, Ellis Horwood, Chichester, 1989, pp. 147, 208.
[13] S. Piperaki, S.G. Penn, D.M. Goodall, J. Chromatogr. A 700 (1995) 59.
[14] J. Szemán, K. Ganzler, J. Chromatogr. A 668 (1994) 509.
[15] P.D. Grossman, J.C. Colburn (Editors), Capillary Electrophoresis—Theory and Practice, Academic Press, San Diego, CA, 1992, p. 337.
[16] H. Engelhardt, W. Beck, T. Schmitt, Kapillarelektrophorese—Methoden und Möglichkeiten, Vieweg, Braunschweig, 1994, p. 139.
[17] S.A.C. Wren, J. Chromatogr. 636 (1993) 57.
[18] W.L. Hinze, Sep. Purif. Methods 10 (1981) 159.
[19] S.M. Han, N. Purdie, Anal. Chem. 56 (1984) 2825.
[20] Y.Y. Rawjee, R.L. Williams, G. Vigh, J. Chromatogr. A 652 (1993) 233.
[21] S.A.C. Wren, R.C. Rowe, J. Chromatogr. 603 (1992) 235.
[22] S.A.C. Wren, R.C. Rowe, J. Chromatogr. 609 (1992) 363.
[23] H. Engelhardt, W. Beck, T. Schmitt, Kapillarelektrophorese—Methoden und Möglichkeiten, Vieweg, Braunschweig, 1994, pp. 145–146.